EPJ Web of Conferences **117**, 07017 (2016) DOI: 10.1051/epjconf/201611707017
NN2015

Sensitivity of N/Z ratio in projectile break-up of isobaric systems

E. De Filippo[1], A. Pagano[1], P. Russotto[1], L. Acosta[2], L. Auditore[3], V. Baran[4], T. Cap[5], G. Cardella[1], M. Colonna[2], L. Francalanza[6], B. Gnoffo[1], G. Lanzalone[7,2], I. Lombardo[6], G. Marquínez-Durán[8], C. Maiolino[2], T. Minniti[1], S. Norella[3], , E.V. Pagano[2,9], M. Papa[1], E. Piasecki[5,10], S. Pirrone[1], G. Politi[9,1], F. Porto[9,2], L. Quattrocchi[3], F. Rizzo[9,1], E. Rosato[6], A. Trifirò[3], M. Trimarchi[3], G. Verde[1], M. Vigilante[6], K. Siwek-Wilczyńska[5] and J. Wilczyński[10]

[1] INFN, Sezione di Catania, Catania, Italy
[2] INFN - Laboratori Nazionali del Sud, Catania, Italy
[3] INFN, Gruppo Collegato di Messina and Univ. of Messina, Italy
[4] Physics Faculty, University of Bucharest, Romania
[5] Faculty of Physics and Heavy Ion Laboratory, Univ. of Warsaw, Poland
[6] INFN, Sezione di Napoli and Dip. di Fisica, Univ. of Napoli, Italy
[7] Università "Kore", Enna, Italy
[8] Departamento de Fisica Aplicada, Huelva, Spain
[9] Dipartimento di Fisica e Astronomia, Univ. di Catania, Italy
[10] National Centre for Nuclear Research, Otwock-Świerk, Poland

Abstract

The binary break-up of projectile-like fragments in non central heavy-ion collisions follows different decay patterns, from equilibrated emission towards dynamical (prompt) fission. Recently, comparing two systems with different N/Z in the entrance channel, it has been shown that the dynamical emission cross-section is enhanced for the most neutron rich system while the statistical emission cross-section is independent from the isotopic composition. In order to understand this dependence and disentangle it from the initial size of the nuclei, we have studied the two isobaric systems $^{124}Xe+^{64}Zn$ and $^{124}Xe+^{64}Ni$ at 35 A MeV (InKiIsSy experiment), in comparison with the previous studied reactions ($^{124}Sn+^{64}Ni$ and $^{112}Sn+^{58}Ni$) at the same bombarding energy. We present the first results evidencing a striking

similar effect in the dynamical decay as a function of the N/Z of the target for equal size systems.

1 Introduction

In non-central heavy ion collisions at intermediate energies, the reaction dynamics can result in binary products such as excited projectile-like (PLF) and target-like (TLF). An important cross-section is also associated with ternary reactions where the PLF and TLF residues are accompanied by the emission of intermediate mass fragments (IMF) and light charged particles. Light IMFs ($Z < 10$) are produced preferentially in the midrapidity region ranging between the PLF and TLF velocities. An important aspect, in fragments and particles emission, is the fact that they are continuously produced all along the dynamical evolution path of the system, from shortest times (pre-equilibrium, prompt neck rupture emission) to longer time scales in the sequential decay of the PLF or TLF primary fragments [1–5]. The analysis of the reactions $^{124,112}Sn + {}^{64,58}Ni$ at 35 A MeV beam incident energy, have shown a well-defined chronology: light IMFs (Z<9) are likely to be emitted either dynamically on a short time scale (within 50 fm/c) with a prompt neck rupture mechanism or statistically in the sequential decay of the PLF and/or TLF primary fragments. Isotopic properties of the neck fragmentation products have been linked to the symmetry energy term parametrizzation of the nuclear equation of state [5]. In contrast, heavier fragments (Z≥9) are predominantly emitted on a longer time scale (>120 fm/c) and they have been associated either with a massive binary splitting of deformed and excited PLF or TLF ("dynamical fission") or a statistical equilibrated fission decay. These different decay patterns for the PLF break-up are characterized by peculiar angular distributions: an aligned break-up with the recoil velocity of the PLF source in the dynamical emission and an isotropic emission of the fission-like fragments in the PLF reference frame in the sequential statistical decay. It has been shown [6, 7] that while the statistical-sequential emission assumes the same cross section for the two systems as a function of the IMF atomic number Z of the emitted fragments, the dynamical IMF emission cross section is enhanced for the neutron rich system, clearly indicating an isospin effects of the entrance channel sensitive to the density dependence of the symmetry term in the nuclear equation of state. However, a contribution to the observed effect related to the different sizes of the studied systems can not be ruled-out [8]. By using the 4π detector CHIMERA, a new experimental investigation was recently carried out (InKiIsSy, Inverse Kinematic

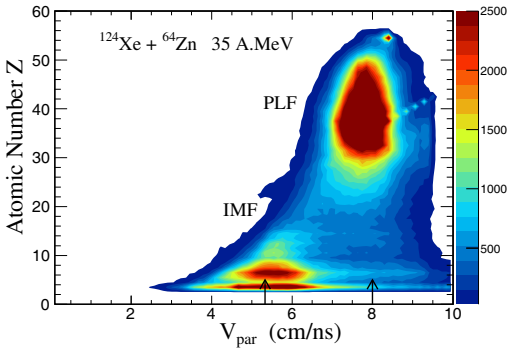

Figure 1: Yield distribution for particles punching-through the Silicon detectors as a function of their atomic number Z and parallel to the beam velocity V_{par}.

Isobaric Systems) at INFN-LNS. Our goal was to extend the previous study, at the same incident energy, using a projectile/target combination having the same mass of the neutron rich system ($^{124}Sn + ^{64}Ni$) and a N/Z close to the value of the neutron poor one, in order to disentangle genuine isospin effects by the ones related to the size of the two interacting systems.

2 Results

The experiment was performed at the LNS Cyclotron facility in Catania using the ^{124}Xe beam at 35 A MeV incident on targets of ^{64}Zn (308 $\mu g/cm^2$) and ^{64}Ni (370 $\mu g/cm^2$) by using the CHIMERA 4π detector. A prototype of the FARCOS correlator array (four telescopes) [9], subtending the polar angles of $15^o \leq \theta_{lab} \leq 45^o$ and the azimuthal interval $\Delta\phi \approx 90^o$, was used for the first time to measure with better angular and energy resolution than in CHIMERA, IMF-IMF and proton-proton correlations for events triggered by the CHIMERA array. In the following, data analysis will be limited to particles well identified in charge by using the $\Delta E - E$ technique in the Silicon-CsI(Tl) CHIMERA telescopes and light charged particles isotopically identified in the CsI(Tl). Future progresses in data analysis will permit to add the particles of lower energies stopped in the silicon detectors and identified in charge and/or mass by Time-of-Flight and Pulse-Shape techniques. A 2-dimensional contour plot of the fragments yields for the $^{124}Xe + ^{64}Zn$ reaction is shown in Fig. 1. In the figure the parallel velocity along the beam axis is correlated with the atomic number. The figure shows the regions of PLF and IMF for well identified events around or above the c.m. velocity. Binary decay of the PLF produced in peripheral reactions were

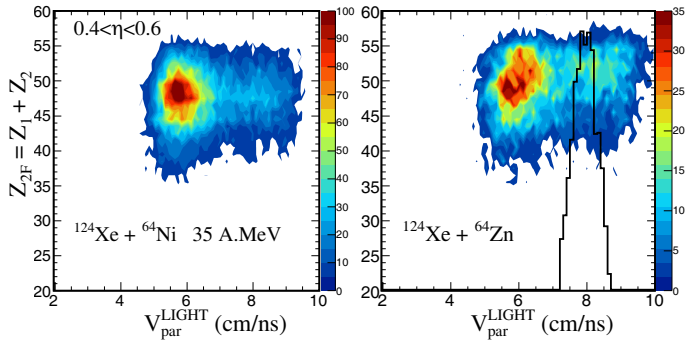

Figure 2: Distribution of the sum of charges of the two heaviest fragments (Z_{2F}) vs. V_{par} of the lighter fragment for ^{64}Ni (left) and ^{64}Zn (right) targets.

selected assuming that the sum of the charge of the two heaviest fragments $Z_{2F} = Z_1 + Z_2$ was larger than the value of 70% of the projectile charge. We show in Fig. 2 the distribution of Z_{2F} vs. the parallel velocity of the lighter fragment for the reactions $^{124}Xe + ^{64}Ni$ (left) and $^{124}Xe + ^{64}Zn$ (right) for a large asymmetric splitting of quasi-projectiles, $0.4 < \eta < 0.6$, where $\eta = (Z_1 - Z_2)/(Z_1 + Z_2)$ is the asymmetry parameter and for a window of the total kinetic energy of the two fragments E_{2F} >2700 MeV, so removing in this way the more dissipative collisions. The velocity distribution of the heaviest fragment, centered around the projectile velocity, is shown for comparison in the right panel. We observe that the light fragment velocity has two components characteristic of "forward" and "backward" emission in the PLF frame as compared with the projectile heavy residue velocity distribution centered around the beam velocity, consistent with the scenario of the scattering of the PLF followed by its splitting into two fragments [2, 6]. The largest component is the backward one when the lighter fragment is emitted with a velocity smaller that the heavier fragment, around 6 cm/ns. To better understand this aspect we compute the θ_{prox} angle, defined as the angle between the reconstructed PLF flight direction in the c.m. system and the relative velocity between Z_1 and Z_2 fragments.

Fig. 3 (left) shows the $\cos(\theta_{prox})$ distributions for three different values of the asymmetry parameter η. For the most symmetric splitting of the PLF ($\eta < 0.2$) the $\cos(\theta_{prox})$ spectrum is symmetric around $\cos(\theta_{prox}) = 0$ as expected for an equilibrated process of binary PLF splitting. For large asymmetric splittings, the distribution results from the superposition of a symmetric component and a pronounced peak $\cos(\theta_{prox}) \approx 1$ increasing with the charge asymmetry. This yield enhancement corresponds to a back-

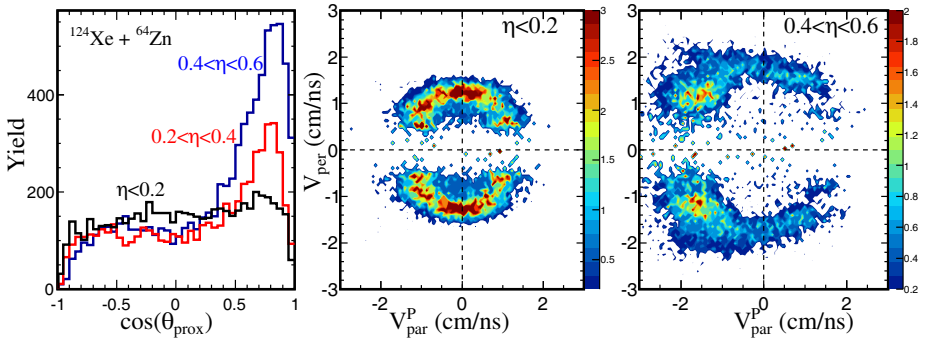

Figure 3: (left) $\cos(\theta_{prox})$ distribution for three different asymmetries η in the binary splitting of the PLF. Invariant cross-sections for the ligher fragment in the reference frame of the PLF for $\eta < 0.2$ (middle) and $0.4 < \eta < 0.6$ (right). Invariant plots are weighted with the fragments transverse momentum $1/p_t$.

ward emission of the fragment, aligned along the direction of the PLF. This anisotropy is one signature of a "dynamical" process [5, 7, 10]. This is confirmed looking at Fig. 3 (right) where the V_{par} vs. the V_{per} Galilean invariant cross-section plot is shown for the lighter fragment in the PLF asymmetric binary splitting in the reference frame of the reconstructed PLF. The forward-backward asymmetry clearly indicates here a component due to a non-sequential emission. This can be compared with the Fig. 3 (middle) plot for symmetric splitting ($\eta < 0.2$) where we observe a typical pattern of a forward-backward symmetry emission around a well defined Coulomb ring expected for an equilibrated break-up. We have used the $\cos(\theta_{prox})$ distributions in order to separate the statistical from the dynamical contribution for the two systems studied here, following the method described in Refs. [6, 7]. In Fig. 4 the ratio of the dynamical component respect to the dynamical+statistical one is shown for the two systems $^{124}Xe +^{64} Ni$ and $^{124}Xe +^{64} Zn$. These preliminary results show clearly that the dynamical component is prevailing for the reaction with a neutron rich target (^{64}Ni). Thus this result indicates independence from the inizial size of the projectile and target.

Extended analysis (including the achievement of data analysis for particles stopping in the Si detectors) and absolute cross sections determination for the statistical and dynamical components, will permit the comparison with results of the previous experiment $^{124}Sn +^{64} Ni$. The dynamical IMF emission is an important mechanism to constraint the density dependence of the symmetry energy but this need calculations that are able to follow the

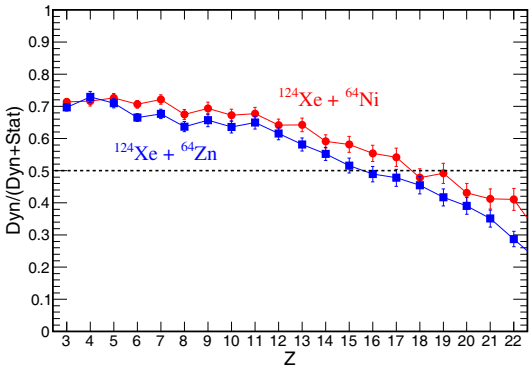

Figure 4: Ratio of the dynamical component vs. the total (statistical+dynamical) as a function of the IMF atomic number for the $^{124}Xe + ^{64}Ni$ (red circles) and $^{124}Xe + ^{64}Zn$ (blue squares) reactions.

largest possible reaction time-scales of the IMF emission. On this light we have started calculations using the Constrained Molecular Dynamics model CoMD3 [11] in order to simulate the two reaction studied here with promising results. Finally the merging of the CHIMERA and FARCOS data will certainly extend our experimental capabilities, due to Farcos enhanced isotopic resolving power for IMFs and light charged particles.

References

[1] E. De Filippo *et al.*, Phys. Rev. C**71**, 044602 (2005); *ibidem* Phys. Rev. C**71** 064604 (2005).

[2] A.B. McIntosh *et al.*, Phys. Rev. C**81**, 034603 (2010).

[3] B. Davin *et al.*, Phys. Rev. C**65**, 064614 (2002).

[4] S. Piantelli *et al.*, Phys. Rev. C**74**, 034609 (2006).

[5] E. De Filippo *et al.*, Phys. Rev. C**86**, 014610 (2012).

[6] P. Russotto *et al.*, Phys. Rev. C**81**, 064605 (2010).

[7] P. Russotto *et al.*, Phys. Rev. C**91**, 014610 (2015).

[8] G. Giuliani *et al.*, IWM2007 Proc., ed. SIF Bologna, Vol. 95, 311 (2008); M. Papa et al., Phys. Rev. C**75**, 054616 (2007).

[9] E.V. Pagano, proceedings of this conference; Technical Design Report - TDR/INFN for the Farcos project: *https://192.84.151.50/joomla*

[10] S. Hudan *et al.*, Phys. Rev. C**86**, 021603 (2012).

[11] M. Papa, Phys. Rev. C**87**, 014001 (2013).